

# **MSM White Paper: Cell Scale to Macroscale Integration**

**Ching-Long Lin<sup>1</sup>, George Karniadakis<sup>2</sup>, James G. Brasseur<sup>3</sup>,**

**Bridget S. Wilson<sup>4</sup>, and Yi Jiang<sup>5</sup>**

**<sup>1</sup>University of Iowa, <sup>2</sup>Brown University, <sup>3</sup>Pennsylvania State University,**

**<sup>4</sup>University of New Mexico, <sup>5</sup>Los Alamos National Laboratory**

## **Table of Contents**

- I. Introduction
- II. Generic Definitions of “Model,” “Computer Simulation,” and “Multiscale Modeling”
- III. Multiscale Nature of Human Bodies
- IV. Recommendations
- V. Goals and Tasks

## I. Introduction

This white paper aims to present numerical methods that facilitate integration of subcellular and cellular scale to macroscale in the human body, and identify associated multiscale modeling issues from the numerical standpoint. Due to the complexity of the human body, the strategies for model integration may be quite different depending on specific problems. Therefore, several examples of multiscale model integration are provided in the appendices A-D.

- A. Airway defense system (3 scales): 3D-1D coupled macro-microscale airway tree system (at organ level), image-driven technique (global) and fluid-structure interaction (local) for a breathing lung, and epithelial cell model for biochemical signaling pathways that regulate water volume for cilia beating and airway clearance. The integrated multiscale model allows simulation and prediction of airway defense system in health and diseased lungs.
- B. Cerebro-vasculature (3 scales): 3D-1D coupled macro-microscale intracranial arterial tree system (at organ level), fluid-structure interaction, and dissipative particle dynamics (DPD) for red and white blood cells. The integrated multiscale model allows study of the processes of initiation, growth and rupture of cerebral aneurysms.
- C. Gastrointestinal tract (2 disparate motility scales plus nutrient transport): advanced lattice Boltzmann algorithms were applied to: (1) macro-scale intestinal flow (2D and 3D), (2) 2D and 3D models of the interactions among between macro-scale eddying flow and a micro-mixing layer generated by the motions of micro-scale finger-like villi along the mucosal surface, (3) a fully coupled 3D model of the enhancement of nutrient transport from the macro-micro scale interactions in the intestine with finger-like villi on the intestinal surface. These simulations have been combined with an image-based study of macro-scale motility in the rat intestine using time-resolved magnetic resonance imaging. The basic physics of nutrient transport from the bulk flow to the mucosal surface from the interactions between highly disparate scales of macro and micro scale motility were studied and the characteristics of villi motion that are required to enhance absorption were deduced. Quantifications of the hydrodynamic environment in the intestine from these models have been subsequently applied to studies of drug dissolution. .
- D. Tumor growth (3 scales): an intracellular model for signaling pathways that determine cell cycle, a cell model at the cellular level using a discrete Monte Carlo method (aka cellular Potts model, extended large-Q Potts model and Glazier-Graner-Hogeweg or GGH model; a lattice-based method to simulate the collective behavior of cellular structures) for cell migration, growth, proliferation, cellular adhesion, and extracellular matrix degradation, and a continuum partial differential equation-based model for extracellular environment to describe diffusion, uptake, and decay of signaling molecules and metabolite. The model integration at the intracellular, cellular, and extra-cellular levels allows prediction of tumor growth and tumor-induced angiogenesis.

Through these examples, several common themes on numerical methods and modeling strategies emerge for discussion. They are:

1. Fluid-structure interaction (FSI)
2. Image-registration driven simulation
3. 3D-to-1D model coupling and interface conditions
4. Combining continuum-mesoscale-atomistic-level simulation

5. Interface and boundary conditions: accuracy and dynamical importance
6. Multiscale geometry representation and boundary conditions
7. Integration of imaging data with modeling and computer simulation
8. Direct vs. indirect interactions between processes that operate at disparate scales
9. Uncertainty in materials properties and geometry
10. Sensitivity and uncertainty in multiscale and multiphysics integration
11. Cell models

One major objective of this white paper is to discuss the advantages, limitations and prospects of different numerical methods and modeling strategies and their integrations for predicting integrative physics and physiology that take place at disparate scales. The ultimate goal of the white paper is to advance the development and application of multiscale methods for the study of biological problems where multiscale interactions are important, and to facilitate national and international collaborations.

## II. Generic Definitions of “Model,” “Computer Simulation,” and “Multiscale Modeling”

### Definitions:

**Model:** the representation of a physical process of interest with another (e.g., mathematical model in physical science or animal model in medical science).

**Mathematical Model:** Mathematical representations of dynamical processes within physical systems based on the laws of physics and combined with empirical data.

**Computer Simulation:** Production of data on computer systems from numerical methods applied to the solution of mathematical representations of dynamical systems based on the laws of physics and combined with empirical data.

**Multiscale Modeling:** mathematical modeling or computer simulation involving the coupling of dynamical processes that occur at disparate scales (i.e., scales that differ by at least an order of magnitude).

### Scales:

The basic molecular to continuum regimes of fluid flow are based on the separation between length scales in the flow  $h$  relative to the mean free path  $\lambda$ , the average distance between molecular collisions. The Knudsen number  $Kn = \lambda/h$  roughly defines the following regimes: .

$$Kn \leq 10^{-2}, \text{ continuum flow}$$

$$10^{-2} \leq Kn \leq 0.1, \text{ slip flow}$$

$$0.1 \leq Kn \leq 10, \text{ transitional flow}$$

$$O(10) \leq Kn, \text{ free-molecular flow}$$

The relationships between  $Kn$  and  $h$  of some flow devices are shown in Fig. 1.

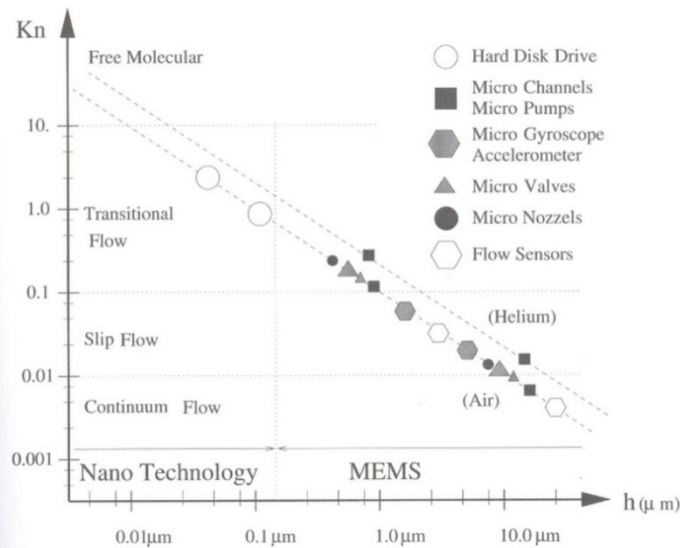


**Figure 1:** Typical MEMS and nano technology applications in standard atmospheric conditions span the entire  $Kn$  regime. “ $h$ ” is the characteristic length scale for the flow (from “Micro Flows” by Karniadakis and Beskok, Springer, 2002).

### Numerical methods:

Depending on the time and length scales of a process/system, different numerical methods have been adopted for simulation as illustrated in Fig. 2. These methods can be classified by one of the three theories (or regimes): continuum-level methods (finite difference, finite volume, and finite element methods), mesoscopic methods (lattice Boltzmann, dissipative particle dynamics and Monte-Carlo methods), and atomistic methods (molecular dynamics). There is currently a need to integrate across methods to accommodate multiscale dynamics and statistics. These theories can be based in an Eulerian, Lagrangian or Eulerian-Lagrangian combined framework to describe the deterministic and/or stochastic nature of the process.

In the continuum regime (e.g. for flow with  $Kn \leq 10^{-2}$ ), finite difference method, finite volume method, and finite element method can be applied to discretize partial differential equations (PDE), ordinary differential equations (ODE), or integral form of mathematical governing equations. The continuum theories are based on physical principles, such as conservation of mass, Newton’s second law of motion, and conservation of energy. The methods in this regime can be regarded as macroscale methods.

Mesoscale methods are based on the concept that coarse-graining can provide an intermediate bridge between continuum and molecular dynamics (MD) modeling strategies. In a Lagrangian framework a coarse-grain particle represents a group of molecules, whereas in an Eulerian framework a particle distribution function is assigned to a lattice point in phase space. Mesoscopic methods are based on rules for motions and interactions of coarse-grain particles or particle distribution functions that must be grounded in the laws of physics. Some mesoscale methods and their features are:

- Lattice Boltzmann Methods (LBM): fixed grid (lattice), particle distribution functions, rules of streaming and collision based on a discretization of the continuous Boltzmann equation from which the continuum level conservation laws can be derived.
- Dissipative Particle Dynamics (DPD): no grid, tracking individual particles, Newton's second law of motion for particle, inter-particle energy potential (Hamiltonian) for particle interactions.
- Monte Carlo method (MC): fixed grid (lattice), Hamiltonian, rules of random (stochastic) process (requiring generation of random numbers), indirect empirical application of the laws of mechanics.

Microscale methods deal with motions and interactions of individual molecules/particles/cells.

At microscopic and mesoscopic levels, individual particles are viewed as discrete entities and their behaviors are regarded as a sequence of discrete events, exhibiting stochastic natures. When applying these microscale/mesoscale methods to simulate physical phenomena at macroscopic levels, an important requirement is for these methods to recover governing PDEs or physical laws at the continuum regime. In the examples presented in appendices, DPD, LBM and MC are applied to simulate red blood cells (appendix B), cavity-villi interactions in gastrointestinal tract (appendix C), and tumor cells (appendix D), respectively. For the airway defense system, the epithelial cells lining the airway wall are not physically modeled because they are stationary, sitting on basement membranes, although they may be subject to stretching and compression of mechanical forces. With the relationship between stress and ATP release measured from the cell culture experiment, the airway epithelial cell model can model intracellular biochemical processes and signaling pathways at molecular level.

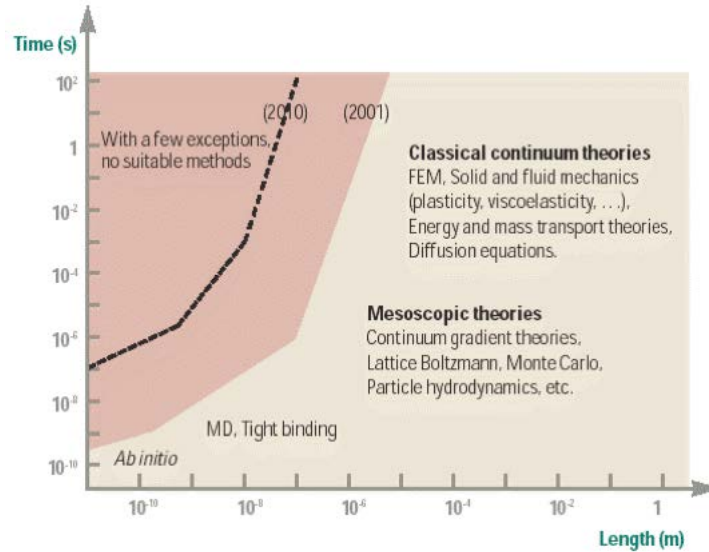


**Figure 2:** Numerical methods for different time and length scales (from Gao, H., *Modelling Strategies for Nano- and Biomaterials*, “European White Book on Fundamental Research in Materials Science”, Max-Planck-Institut, Germany, 2001).

When applying the above numerical methods to PDEs, physical principles or theories that govern the system, we obtain a model.

### III. Multiscale Nature of Human Bodies

In order to move toward a true Physiome, we need to understand and integrate across disparate scales within the structure and function of the human body at all levels, including the organ level, the tissue, the cellular level, and the molecular level. Multiscale phenomena occur across all levels and certain multiscale interactions play key roles in function and their disruption in disease. An example of key components linking scales in the same level and across levels are stress transmission and mechanotransduction (one form of signal-transduction; note that the majority of signal transduction is mediated by signaling molecules). For example, Fredberg and Kamm (2006) elucidated in a review article about multiscale phenomena in the lung that “The pathway for force transmission [by application of physical forces on the macroscale and their transmission to the scale of small airways] then continues down to the level of cell, nucleus, and molecule: moreover, to lesser or greater degrees most cell types that are resident in the lung have the ability to generate contractile forces. At these smallest scales, physical forces serves to distend the cytoskeleton, drive cytoskeletal remodeling, expose cryptic binding domains, and ultimately modulate reaction rates and gene expression.”

Another example is neuromuscular physiology where neuronal activity at the cellular level directly controls activity in the muscles at the tissue level. Whereas neural control is based on chemical

transport and kinetics at the molecular scale, the response to neural stimuli at the tissue level integrated directly with the generation of mechanical stresses within muscle structures at the macro scale, and has a direct impact on function, dysfunction, and disease. Indeed, it is at this level that the connection with medical science, particularly clinical medicine, often occurs.

Ingber (2003) and Tschumperlin and Drazen (2006) had also recognized the importance of integrating mechanics into understanding of the molecular basis of disease. That is, mechanical forces (resulting from the movement of our bodies) are transmitted from macroscale to microscale at organ level and across levels to cellular level. Cells then sense and respond to mechanical stress (aka. cellular mechanotransduction that converts a mechanical stimulus to biochemical process). A wide range of diseases are resulted from abnormal mechanotransduction in response to abnormal mechanical stress and subsequent intracellular/subcellular reactions.

**References:**

Fredberg, J. J. and R. D. Kamm, Stress Transmission in the Lung: Pathways from Organ to Molecule. *Annu. Rev. Physiol.* 68:507-541, 2006.  
 Ingber, D. E., Mechanobiology and Diseases of Mechanotransduction. *Ann. Med.* 35(8): 564-577, 2003.  
 Tschumperlin, D. and J. M. Drazen, Chronic Effects of Mechanical Force on Airways. *Annu. Rev. Physiol.* 68:563-583, 2006.

**IV. Recommendations**

Current multiscale methods:

The multiscale modeling methods adopted by the four projects presented in the appendices are summarized in a table below. “x” in the table means that it is used as explained in appendices.

Scale	Macroscale to extra-cellular level								Mesoscale cellular level	Microscale intracellular level
Methods	Global	Local	Fluid		Solid		FSI		Collective structural behavior	Biochemical signaling pathways
Geometry	Organ scale	Part of organ	Subject-specific prediction	General predictions	Subject-specific predictions	General predictions	1 way coupling	2 way coupling		
Lung	3D3D, 3D1D	3D	FEM		FEM		IR	FEM	cell culture experiment	x
Blood	3D1D	3D	FEM		FEM			FEM	DPD	
GI tract (gut)	2D 3D LBM, organ scale	2D 3D LBM		LBM			x			
Tumor	x	x		x	x	x		x	MC, rule	Boolean, rule-based

The key to achieve an integrative Physiome lies in our ability to modeling (multiscale) stress transmission in the same level and across levels and mechanotransduction at cellular level.

To accurately model stress transmission and transport starting at the organ level, accurate time-dependent quantifications of anatomy at the organ and tissue levels with detailed individualized geometrical features in a dynamic setting are needed. The approaches of 3D-3D (large-scale 3D structures coupled with small-scale 3D ones) and 3D-1D (large-scale 3D structures coupled with small-scale 1D ones) are adopted. To model mechanical forces in a living system, both fluid (air, blood and gastrointestinal flows) and solid (tissue and extracellular matrix) and their interactions are modeled. Whereas in some models the space-time changes in fluid boundaries are obtained from imaging data, other models integrate fluid-structure interaction (FSI). Whereas image data are often used to describe average geometry behaviors, image-registration (IR)-based simulation is also being employed. To accurately predict the sequences of intracellular/subcellular events associated with mechanotransduction, it is necessary to model the mechanical stress in the setting of cell microenvironment, that is why cell culture experiment, DPS and MC are used in different applications. Intracellular modeling is aimed at understanding the mechanotransducing mechanism.

#### Issues and recommendations:

##### 1. Education:

To achieve a better integrative Physiome, computational scientists and engineers need to learn more about mechanobiology. Likewise, biologists and medical scientists need to be better educated in the application of the laws of mechanics and about mathematical and computer modeling methods.

We recommend that NIH sponsor short courses/summer workshops offered through NIH sponsored centers and leading institutions by inviting instructors/speakers/attendees worldwide in various disciplines, including basic mechanics, computational science/engineering, mechanobiology, physiology, medicine, imaging, geometric modeling, and among others.

##### 2. Imaging and Geometric Modeling:

Structure determines function, and function may alter structure. To understand structure-function relationship at all levels, we need to improve the accuracy of imaging, image analysis and geometric modeling of structure, and to quantify the uncertainty of geometric models and its effect on function. Examples include the airways and vessel trees or subcellular and cellular structures. In many applications dynamical changes with time are central, but space-time imaging and image analysis is not as far advanced as is static imaging. Examples include the gastrointestinal and cardiac function.

We recommend that NIH promote study of image-based morphology at the organ and tissue functional levels, and the integration of imaging data into modeling strategies. Specific focuses should be placed on space-time imaging and image analysis, and on uncertainty and the statistical quantification of inter and intra subject variability in health and disease.

3. Transport within Biofluid Flow Simulation:

Transport within biological fluid flows occurs over an extremely wide range of scales and with complexity that includes critical interactions at the cellular level and transport at the molecular level within continuum level bulk flow. To study multiscale interactions in association with fluid flow, we recommended that emphasis be directed at the accuracy of bio fluid flow simulation at different scales and that empirical and approximate modeling strategies be progressively replaced by more exact methods grounded in the laws of physics and with the lowest reasonable level of parameterization. In this way more modeling and computer simulation will be directed, over time, to become increasingly physiologically relevant.

4. Tissue Properties and Multiscale Tissue Mechanics:

Tissues properties *in vivo* are lacking. More quantitative experimental measurements of cell and tissue level behaviors and properties are needed to establish baseline model parameters and to validate simulation results. These properties are important in modeling fluid-structure interaction for stress transmission and for neuromuscular controls. We recommend that NIH encourage and support the development of new methods for quantifying tissue properties and modeling multiscale tissue mechanics that can address *in vivo* as well as *in vitro* response.

5. Uncertainty Quantification:

We recommend that NIH emphasize the quantification of uncertainties in tissue and fluid properties, geometrical modeling, model parameterization, constitutive laws, or model boundary condition, and the impact of such uncertainties in multiscale and multiphysics integration.

6. Development of New Mathematics for Multiscale Biological Modeling:

We have standard techniques to solve and analyze PDEs, but we don't have the equivalent for the rapidly growing field of mathematical/computational biology. In particular the state-of-the-art multiscale models in biology are at present more like art and magic than rigorous mathematics. The long-term goal would be to enable the next generation of students and researchers to pick up textbooks and learn methods to analyze multiscale models like we can now with PDEs.

### Future direction of health care:

Applications of multiscale models are expected to include improved ability to, for example, detect the onset, progression, extent and location of functional and structural disorders at all levels of human bodies.

With the mapping of the human genome essentially completed, and we contemplate modification of the very genetic nature of disease and disease susceptibility, we must have sensitive, quantitative methods that can rapidly assess and further predict subclinical phenotypic outcomes. This is particularly difficult when pathologic changes are slow to develop, heterogeneous, and multiple pathologic processes intermingle. Understanding and prediction of (fluid and tissue induced) mechanical stress in an individual subject's anatomy and the pathways for their transmission from organ to molecule allow us to understand pathogenesis and progression of disease at the most basic level, and possibly use the model to design and test novel molecular therapeutics for diseases. This personalization of medicine through imaging and associated value-added high level modeling is determining the direction of health care in the next decade, and adds additional meaning to genotypic patient specific descriptors.

### **V. Working Group Goals and Tasks**

1. Publication: Special issues on multiscale modeling in high-quality, high-impact archival journals, e.g. Journal of Computational Physics.
2. Conference: Joint U.S. IMAG MSM and Euro VPH meeting (2011): seek financial support from NIH and NSF or others.
3. Collaboration: Promote collaborations between WG members (through grant applications) to build a more integrative model toward Physiome.

## Appendix A:

### Modeling of Airway Defense System in the Human Lung by Ching-Long Lin

#### I. Need for an Integrated Cell-Mechanics Model

Airway defense is a multiscale process, involving mechanotransduction to transmit oscillatory mechanical force from macro scale (motion of lung, rib cage, diaphragm, and abdomen) to micro scale (airflow-induced shear stress and tissue stress at a local level), and further translation to biochemical responses via cell signaling to maintain the periciliary liquid (PCL) volume for mucociliary clearance. Lung diseases may alter mechanical force, which then alters *stress-mediated* adenosine triphosphate nucleotide (ATP) release, disturbs PCL water homeostasis, and weakens the integrated airway defense system, forming a vicious cycle of events. Airway bifurcation is particularly sensitive and vulnerable to the above pathologic process because local maximum stress is located in the vicinity of the bifurcation and increases substantially with airway stiffening and narrowing as found in the diseased lungs so that it can easily exceed the normal physiological range of stress. In the healthy lung, PCL and mucus - together with trapped inhaled bacteria and particulates - are continuously transported cephalad by coordinated ciliary beating. The bifurcation is a singular point where the inner walls of daughter branches meet and toxins/irritants accumulate; this is therefore a key weak spot in the network of mucociliary transport. A failure to maintain PCL water homeostasis near the bifurcation might effectively disrupt this defense pathway.

In order to understand the relationship between mechanical forces at the organ level and cell responses at the cellular level and model the airway defense system, the systems biology approach that integrates mechanics and cell models is needed. The mechanics model utilizes imaging-based, high-fidelity fluid-structure interaction (FSI) computational technologies for three-dimensional (3D) fluid and solid mechanical systems to predict airflow-induced shear stress and tissue stress at a local level in the realistic human lung models. The cell model is based upon mathematical cell biology and *in vitro* data for epithelial cells and nucleotide metabolism to predict ATP release, cell metabolism, ion and water transport, PCL height, and calcium ion concentration [ $\text{Ca}^{2+}$ ]. The stress computed from the mechanics model is used as an input for the cell model. The predictions by the cell model, such as PCL height and [ $\text{Ca}^{2+}$ ], can be mapped to the 3D airway geometry to study the interaction between lung and cells and its role in the distribution and progression of lung disease.

## II. Critical Link Between Scales: Cellular Response to Mechanical Force

The human bronchial epithelial (HBE) cells, like other cell types (e.g., endothelia), have mechanosensing capabilities that can detect changes to the extracellular micromechanical environment. The mechanical force exerted on the lung to change lung volume and pulmonary airflow can be transmitted from the organ level down to the levels of tissue, cell and molecule. From HBE cell culture experiments, Tarran *et al.*, (2005, 2006) and Button *et al.* (2007, 2008) found that HBE cells respond to mechanical force. Figure 1 shows that the epithelial cells release ATP into the PCL in response to: (1) airflow-induced oscillatory shear stress and (2) (transepithelial) cyclic compressive stress (CCS). Here oscillatory (or phasic, cyclic as opposed to static) indicates inspiration/expiration of the airflow and expansion/recoil of the lung. CCS mimics the transmural airway pressures of tidal breathing. Their major findings are: (1) HBE ATP release only responds to phasic motion, (2) the ATP release increases with increasing stress, but quickly reaches a plateau. These findings suggest that the rate of change of stress, not just its magnitude alone (due to phasic motion), is the important stimulus for ATP release into the extracellular PCL environment. ATP, along with its metabolite adenosine, interact with airway epithelial purinergic receptors, to up-regulate transcellular ion and water transports that increase PCL volume and ciliary beat frequency to accelerate mucus transport. HBE cells also protect themselves from over-stimulation and flooding of the airways by limiting ATP release during non-physiological stresses (refer to the plateau in Fig. 1). Thus, beyond the physiological range of stress, ATP release rates become less sensitive to higher stresses applied.

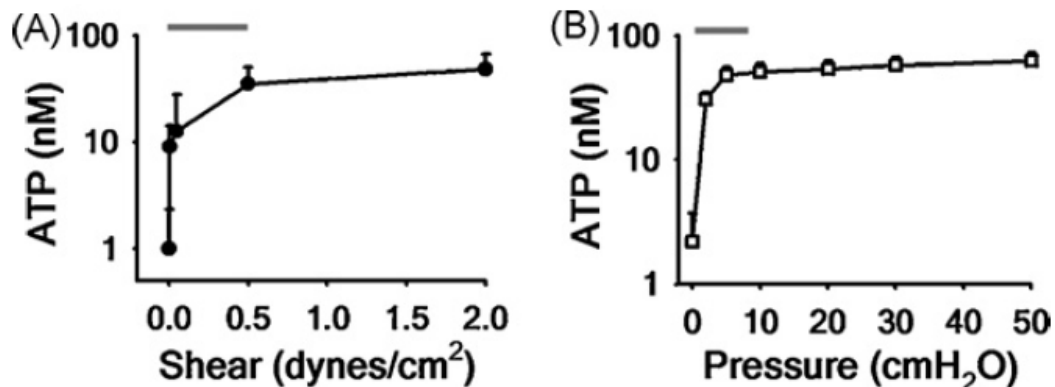


**Figure 1:** Release of ATP during physiological stress. Relationship with magnitude of oscillatory (A) shear stress and (B) compressive stress. Red lines denote the physiological range of stress during tidal breathing (Button *et al.*, 2007, 2008).

### III. Cell Model

In healthy subjects the PCL extends from the cell surface to a depth equal to the length of an out-stretched cilium. The cilia beat in a coordinated fashion at  $\sim 7\text{Hz}$ . If the PCL layer is not maintained at an adequate depth the cilia may become entangled in the mucus, and unable to disengage in the recovery stroke, resulting in no net movement of mucus. Conversely, if the PCL layer is too deep the cilia may be unable to contact the mucus to apply force. It is therefore imperative that ASL hydration is maintained within a specific tolerance, and hence it is one of the most tightly regulated microenvironments within the body. To maintain the optimal PCL depth of  $\sim 7\mu\text{m}$ , water movement into and out of the lumen is regulated through active ion transport. Normal airway epithelium has the capacity to absorb and secrete salt, predominantly  $\text{Na}^+$  and  $\text{Cl}^-$ , thereby generating osmotic gradients which induce water flow across the epithelium. Figure 2 shows a schematic diagram of the mechanism by which ion channels, pumps, and cotransporters establish an osmotic gradient to drive water flow (Warren *et al.*, 2009, 2010). The epithelial  $\text{Na}^+$  channel (ENaC) serves as the major conduit for  $\text{Na}^+$  through the apical membrane, and the  $\text{Na}^+-\text{K}^+-\text{ATPase}$  is the mechanism of basolateral extrusion. Transport of  $\text{Cl}^-$  through the apical membrane is primarily through the CFTR and the  $\text{Ca}^{2+}$ -activated  $\text{Cl}^-$  Channel (CaCC).

Under a number of stress conditions airway epithelial cells release nucleotides into the lumen (see Fig. 2). Nucleotides act as signaling molecules to activate cell surface receptors, and are then degraded via ecto-nucleotidase activity. The  $\text{P2Y}_2$  receptor plays an important role in this autocrine response.  $\text{P2Y}_2$  receptors are G-protein coupled receptors (GPCRs), which act through the Gq/Phospholipase C pathway to produce the cytosolic signaling molecule  $\text{IP}_3$  (inositol-triphosphate, a secondary messenger). Cytosolic  $\text{IP}_3$  binds to Endoplasmic Reticulum (ER) receptors, triggering the release of calcium from the ER into the cytosol. Intracellular  $\text{IP}_3$  concentration is known to be calcium dependent and this feedback is responsible for the characteristic oscillations of  $[\text{Ca}^{2+}]$  concentration within the cytosol. The rise in  $[\text{Ca}^{2+}]$  within the cell also activates CaCCs and Calcium-activated potassium channels (CaKCs) causing an osmotic gradient to form across the epithelium, which results in a flux of water into the lumen.

We plan to adopt a mathematical model that predicts PCL height and  $[\text{Ca}^{2+}]$ , i.e. disruption from PCL volume homeostasis leading to an intracellular  $\text{Ca}^{2+}$  transient reaction, in response to stress-mediated ATP release (Warren *et al.*, 2009, 2010). The model has been compared against the experimental calcium traces of the rabbit tracheal epithelial cells upon stimulation with 0.1, 1, and 2  $\mu\text{M}$  ATP (Zhang *et al.*, 2003). The model predicts similar  $[\text{Ca}^{2+}]$  oscillatory behaviors and pulsatile change of PCL height.

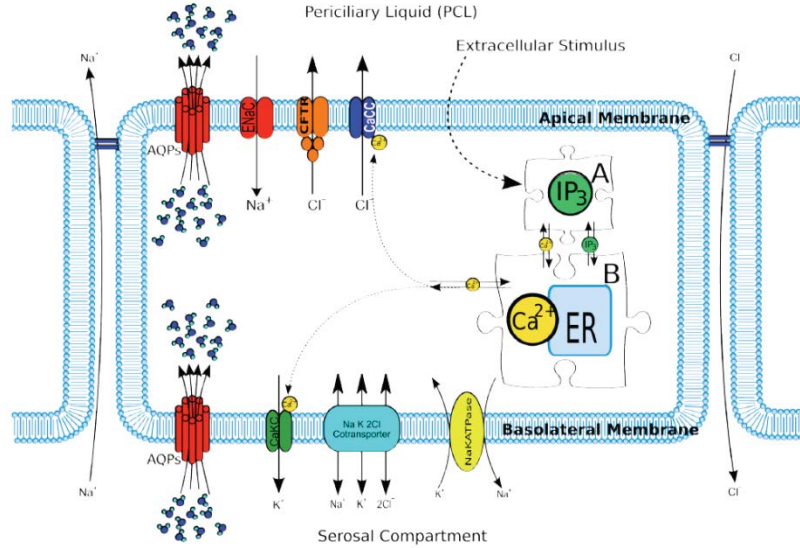


**Figure 2:** Schematic of epithelial model components (Warren et al. 2009), showing the production of IP<sub>3</sub> after being triggered by an extracellular stimulus, the regulation of the inositolphosphate pool, and Ca<sup>2+</sup> handling of the cell activated through IP<sub>3</sub>. AQPs, aquaporins.

#### IV. Mechanics Models

One-way and two-way FSI mechanics models (Choi et al., Lin et al., Tawhai et al., Xia et al.) may be adopted to predict stress distributions in the human lungs. In the one-way FSI approach, the fluid (CFD) and solid (CSM) solvers are executed separately (Fig. 3). The boundary surface meshes between fluid (pulmonary gas flow) and solid (lung tissue mechanics) domains and the lobar and vessel tree boundary meshes are deformed using the image-registration derived displacement fields. The airway and lobe deformations are determined *a priori* to match as precisely as possible with CT images at different lung volumes (Yin et al.), and then are provided to both solvers as Dirichlet boundaries. In the two-way FSI approach (Fig. 4), the FSI interface between fluid and solid domains now are treated as internal nodes, and their positions and velocities are computed from the interactions between pulmonary gas flow and lung tissue mechanics. Any disagreement between the deformed airways (or the displacements of lung tissues) and those derived from image registration indicates that the FSI model has flaws caused by either prescribed lung biomechanical properties for CSM or lack of incorporation of detailed physiological processes into the model. A comparison between two-way and one-way FSI solutions allows identifying the potential source of the problem that causes the disagreement. One-way FSI is considered more accurate, but more restrictive, than two-way FSI because the former relies more on measurement data.

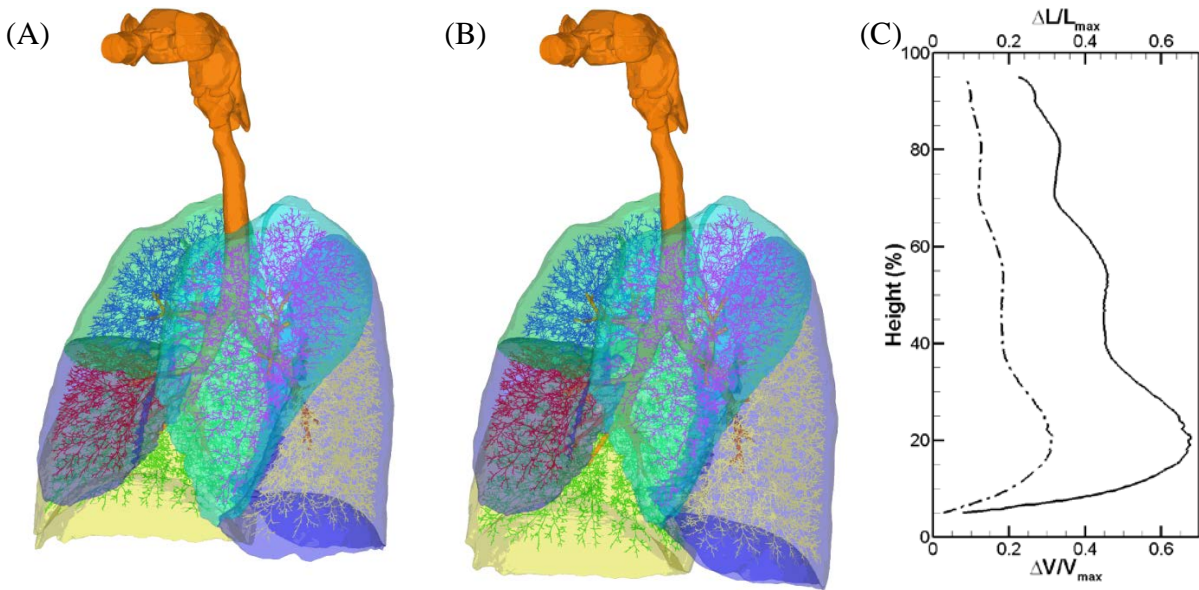


**Figure 3:** 3D-1D coupled airway tree and five lobes at (A) the minimum volume (55% VC) and (B) the maximum lung volume (85%VC). (C) The distribution of deformation as a function of normalized lung height from the apex (100%) of the lung to the base (0%) calculated from the Jacobian.  $\Delta V$  and  $\Delta L$  denote volume and length changes. The subscript “max” corresponds to the maximum lung volume. Tawhai and Lin (2010)

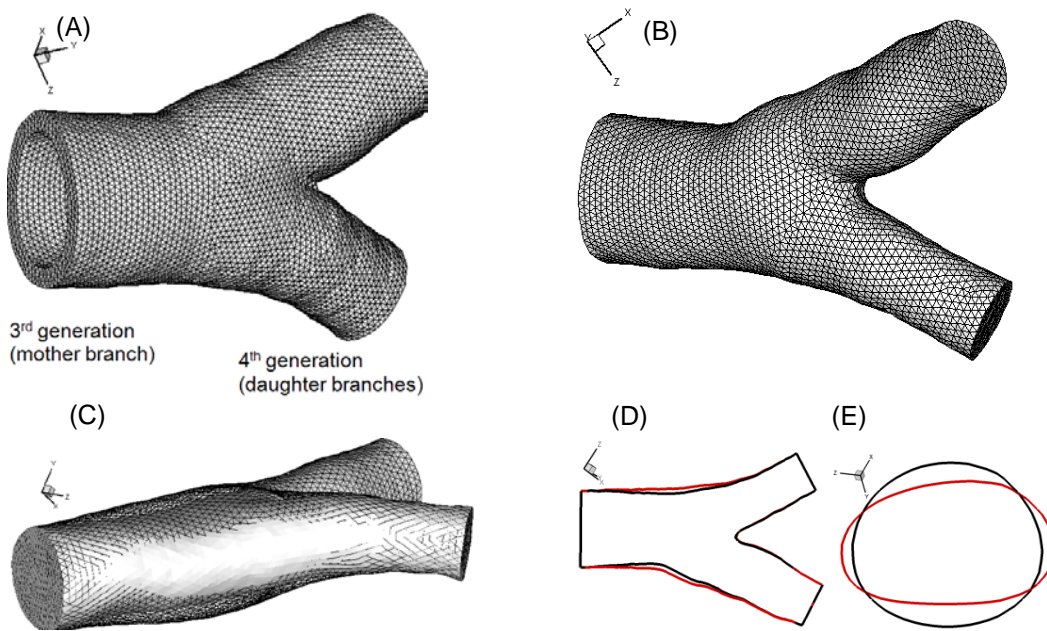


**Figure 4:** Meshes of a CT-based airway bifurcation: (A) wall, (B) lumen. (C) Volume change of the lumen between peak inspiration (wireframe) and resting state (gray) at  $Re=183$ . Deformation in: (D) the bifurcation plane, and (E) the transverse plane before bifurcation (black, maximum deformation; red, resting state). Xia et al. (2010)

## V. Methods and Integration

A key component in the airway-defense system is “stress-mediated ATP release” that interconnects three scales: pulmonary airflow at the organ scale (which exerts shear stress on the airway liquid lining the epithelia), tissue tensile force at the tissue scale (which produces CCS on the epithelia), and epithelial cell response and signaling at the cellular/molecular scale (which releases ATP in response to cyclic stresses).

With the relationships between stress and ATP-release measured from cell culture experiments (Fig. 1), accurate prediction of ATP release (output), which up-regulates cell signaling and reaction to maintain PCL volume and hydration, relies upon accurate prediction of stress (input) that triggers its release in a location-specific and state-specific manner. Therefore, the stress computed from the mechanics model will be used as an input for the cell model. The cell model together with the thermodynamics laws for heat and moisture is then used to predict the biochemical responses of HBE cells and the regional distributions of PCL water level and  $[Ca^{2+}]$  concentration. These predictions can be mapped to the 3D airway geometry to study the interplay between cell and organ.

## VI. Limitation

1. Single versus multiple types of cell models: Mechanical stress may simultaneously affect several cell types that shape and remodel airway structure, and vice versa. Here we only consider HBE cells.
2. Liquid lining, mucus layer, and cilia: The airway surface liquid (ASL) lining covering the epithelia (PCL+mucus layer) is modeled as a compartment with dynamically changing depth; however we do not consider fluid interaction with the cilia in the PCL or the mucin release pathway. Whether cilia act as flow sensors in epithelia to transduce phasic stress is not known. Mucociliary clearance can be modeled by three different approaches: phenomenological, slender body theory, and FSI models (Smith *et al.*, 2007, 2008; Yang *et al.*, 2008), all from the mechanical point of view only.

## VII. References

1. Button, B., M. Picher, and R.C. Boucher. Differential effects of cyclic and constant stress on ATP release and mucociliary transport by human airway epithelia. *J. Physiol.* 580: 577-592, 2007.
2. Button, B. and R.C. Boucher. Role of mechanical stress in regulating airway surface hydration and mucus clearance rates. *Resp. Physiol. Neurobiol.*, 163 (1-3), 189-201, 2008.
3. Choi, J., G. Xia, MH Tawhai, EA Hoffman, and C.-L. Lin, "Numerical study of high frequency oscillatory air flow and convective mixing in a CT-based human airway model," DOI: 10.1007/s10439-010-0110-7, *Annals of Biomedical Engineering*, 2010.
4. Choi, J., M.H. Tawhai, E.A. Hoffman, and C.-L. Lin, "On intra- and inter-subject variabilities of airflow in the human lungs," *Phys. Fluids*, 21, 101901, 2009.
5. Lin, C.-L., M. H. Tawhai, G. McLennan, and E.A. Hoffman, "Multiscale Simulation of Gas Flow in Subject-Specific Models of the Human Lung," *IEEE Eng. in Medicine and Biology*, 28(3): 25-33, 2009.
6. Lin, C.-L., M. H. Tawhai, G. McLennan, and E.A. Hoffman, "Characteristics of the turbulent laryngeal jet and its effect on airflow in the human intra-thoracic airways," *Respir. Physiol. Neurobiol.*, 157: 295-309, 2007.
7. Smith, D.J., E.A. Gaffney, and J.R. Blake. A viscoelastic traction layer model of muco-ciliary transport. *Bulletin of Math. Biology*, 69: 289-327, 2007.
8. Smith, D.J., E.A. Gaffney, and J.R. Blake. Modelling mucociliary clearance. *Respir. Physiol. Neurobiol.* 163(1-3): 178-188, 2008.
9. Tawhai, M. H. and C.-L. Lin, "Airway Gas Flow," *Comprehensive Physiology*, Wiley-Blackwell, in press, 2010.
10. Tawhai, M. H. and C.-L. Lin, "Image-based modeling of lung structure and function," *Journal of Magnetic Resonance Imaging*, in press, 2010.
11. Tawhai, M. H., M. P. Nash, C.-L. Lin, and E. A. Hoffman, "The influence of supine and prone posture on regional lung density & pleural pressure gradients in the human lung", *J. Appl. Physiol.*, 107: 912, 2009.
12. Tawhai, M. H., E. A. Hoffman, and C.-L. Lin, "The Lung Physiome: merging imaging- based measures with predictive computational models of structure and function," *Wiley Interdisciplinary Reviews: Systems Biology and Medicine*, 1(1): 61-72, 2009.
13. Warren, N.J., M.H. Tawhai, and E.J. Crampin. The effect of intracellular calcium oscillations on fluid secretion in airway epithelium, *Journal of theoretical biology* 265(3):270-7, 2010
14. Warren, N.J., M.H. Tawhai, and E.J. Crampin. A Mathematical Model of Periciliary Liquid Depth Regulation in Ciliated Airway Epithelium, *Journal of theoretical biology* 259(4):837-49, 2009
15. Xia, G., M. H. Tawhai, E. A. Hoffman, and C.-L. Lin, "Airway Wall Stiffness and Peak Wall

Shear Stress: A Fluid-Structure Interaction Study in Rigid and Compliant Airways,” *Annals of Biomedical Engineering*, 38(5), 1836-1853, 2010.

16. Yang, X., R. H. Dillon, and L. J. Fauci. An integrative computational model of multiciliary beating. *Bulletin of Math. Biology*, 70: 1192-1215, 2008.
17. Yin, Y., J. Choi, E.A. Hoffman, M.H. Tawhai, and C.-L. Lin, “Simulation of pulmonary air flow with a subject-specific boundary condition,” *Journal of Biomechanics*, 43(11):2159-2163, 2010.
18. Yin, Y., E. A. Hoffman, and C.-L. Lin, “Mass preserving non-rigid registration of CT lung images using cubic B-spline,” *Medical Physics*, 36(9): 4213-4222, 2009.
19. Yin, Y., E. A. Hoffman, and C.-L. Lin, “Local tissue-weight-based nonrigid registration of lung images with application to regional ventilation”, *SPIE Medical Imaging*, vol. 7262, p. 72620C, 2009.
20. Zhang, L. and M. J. Sanderson. Oscillations in ciliary beat frequency and intracellular calcium concentration in rabbit tracheal epithelial cells induced by ATP. *J Physiol (Lond)* 546:733-749, 2003.

## Appendix B: by George Karniadakis

### Need for an Integrated Cerebro-Vasculature Model

The human brain although less than 2% of the body weight, receives about 20% of the resting cardiac output of blood and 25% of body's oxygen supply. Interactions of blood flow in the human brain occur between different scales, determined by flow features in the large arteries (diameter of 0.5 mm or larger), the smaller arteries and arterioles (500 microns to 10 microns), and the capillaries (mean diameter of 5 microns) all being coupled to cellular and sub-cellular biological processes. While many biological aspects have been studied systematically, surprisingly less effort has been put into studying blood flow patterns and oxygen transport within the brain, i.e., the fundamental biomechanical processes of the integrated intracranial vascular network. However, recent pioneering 3D imaging of the human brain by Cassot et al. (2006) and of the mouse brain by Mayerich et al. (2008) provides statistical information for constructing realistic topological models on which future brain simulations will be based. A key observation is that arterioles down to 10 microns follow a tree-like structure (governed by a fractal law) whereas the capillary bed (below 10 microns) follows a net-like structure.

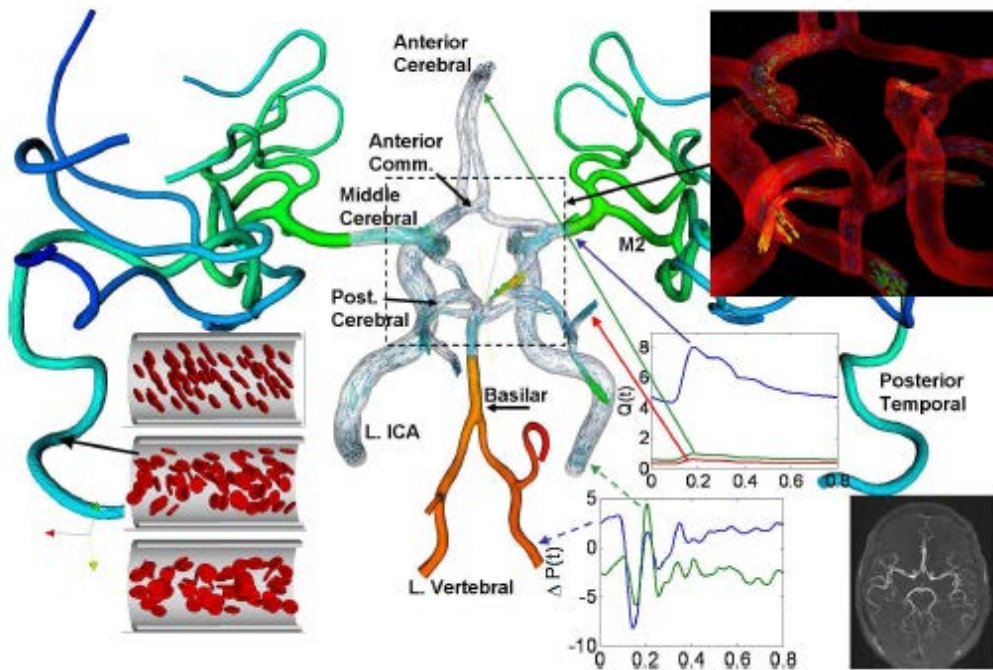


**Figure 1:** *MaN simulations involving a complete Circle of Willis consisting of 65 arteries. Colors represent pressure (inner part is transparent to show velocity vectors and not pressure levels) arrows velocity, XY plots depict flowrate in ml/s and pressure drop in mmHg. Top right: instantaneous streamlines shown swirling flow in communicating arteries. Bottom right: MRA image of the cranial arterial system provided by Prof. J.R. Madsen & Dr. T. Anor (Harvard Medical School).*

Following these observations and based on other clinical results, it is now possible to advance the development of an integrated model of the vascular network in the human brain (cerebro-vasculature) characterized by three distinct spatial length scales (Grinberg et al, 2009):

- (1) The macrovascular network (**MaN**) consisting of large arteries, down to diameter of 0.5 mm, which are patient-specific and can be reconstructed from CT/MR imaging. Typically, about 100 such arteries are involved surrounding the circle of Willis, which is formed downstream of the four main arterial inlets at the neck (two carotids and two vertebral arteries); see Figure 1.
- (2) The mesovascular network (**MeN**) consisting of small arteries and arterioles, from 500 microns down to 10 microns, which follow a tree-like structure governed by specific fractal laws (Cassot et al, 2006; Zamir, 1999). The human brain contains about 10 million small arteries and arterioles.
- (3) The microvascular network (**MiN**) consisting of the capillary bed, which follows a net-like structure; its topological statistics have been recently quantified for the human brain in Cassot et al. (2006). The typical number of capillary segments in the brain is more than 1 billion.

We could study each network separately but there are several reasons for coupling these vascular networks and not simply model MaN as in Figure 1: (1) to provide a closure for MaN modeling, (2) to model brain perfusion in pathological cases, (3) to model neuro-vascular coupling. With regards to (1), outflow boundary conditions have been developed that aim to minimize the effect of not including the MeN-MiN components (see Figure 1 for a healthy case and Grinberg et al., 2009). However, it has been found that in *pathological cases* (e.g., hydrocephalus, aneurysms, etc.) the blood flow circulation depends strongly on the outflow boundary conditions. For example, in a systematic study of brain aneurysms the size effect of the computational domain was examined and differences of up to 100% in wall shear stress (WSS) on the aneurysm were found (Baek et al, 2007). Clinical data can be used at all the outlets but such measurements are extremely difficult and costly. This and other results point to the need for a *closure model*, that is, a full-scale model that couples the macrovascular “image-based” simulations to the “subpixel” simulations involving the mesovascular and microvascular networks as well. This multiscale (MaN-MeN-MiN) brain model will provide the closure conditions. With regards to (2), a full-scale mode will facilitate physiologically correct simulations of brain perfusion and associated pathologies (e.g., malaria, sickle cells anemia, see Kaul & Fabry, 2004 and Chien et al., 1982) for *realistic* studies. In particular, oxygen transport from the red blood cells (RBCs) to the brain takes place primarily at the MiN-MeN levels, and hence these networks have to be explicitly integrated to MaN. Finally, to model the active vaso-dilation of the arteries and arterioles we need to couple it to the neuronal system accounting explicitly for the action of astrocytes on the surface of the vessels.

In summary, the proposed MaN-MeN-MiN is a conceptual framework that can lead to an integrated computational model for the cerebro-vasculature for studying various pathologies in the brain. In the next section we give a specific example of a MaN-MiN coupling, where blood cells and their interaction with the arterial wall need to be modeled explicitly.

## **Specific Example: Multiscale Modeling of Cerebral Aneurysm**

Cerebral aneurysms (CAs) are pathological, blood-filled permanent dilations of intracranial blood vessels usually located near bifurcations in the Circle of Willis (CoW), see Figure 2, see Baek et al. (2010 and references therein). CAs occur in up to 5% of the general population, and can cause subarachnoid hemorrhage (SAH), a devastating event afflicting over 40,000 Americans each year. Over 60% of patients with SAH (a form of stroke) are left dead or disabled, and less than 50% of survivors are able to return to their former jobs or level of activity. The processes of initiation, growth and rupture of CAs are not well understood, and several -- often contrasting - hypotheses on the modified hemodynamics have emerged in recent years, e.g. see the recent reviews in (Lasheras, 2007; Sforza et al, 2009) and references therein.

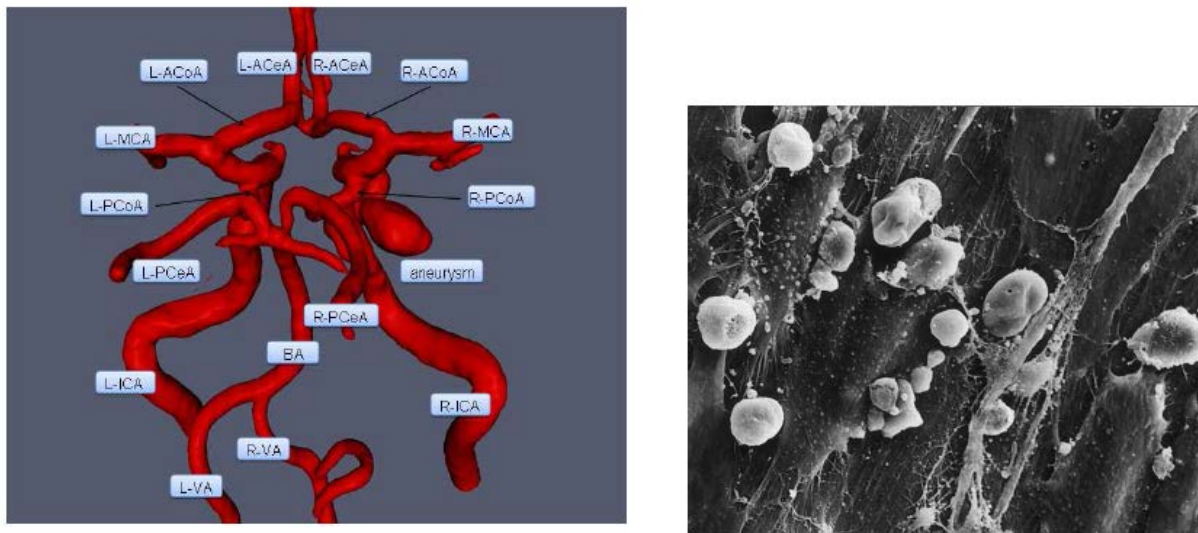


**Figure 2:** Left: Reconstructed intracranial arterial tree of a patient with an aneurysm showing the circle of Willis and all main arteries. ICA: internal carotid; MCA: middle cerebral; VA: vertebral; PCoA: posterior communicating, etc. (Courtesy of Prof. J.R. Madsen and Dr. T. Anor, Harvard Medical School). Right: Scanning electron microscope image of the inside layer of a ruptured MCA aneurysm showing the disrupted pattern of endothelial cells and blood cells adhered to the inter-endothelial cell gaps. (Kataoka et al., 1999).

While one would expect that *aneurysm rupture* be associated with high pressure or high wall shear stress (WSS) magnitude, this is not the case with CAs as no elevated peak pressure and typically low WSS values are observed within the aneurysm. Hence, to advance our understanding, we need to investigate scenarios beyond the pure mechanical point of view. In particular, *we need to understand the role of endothelial cells (ECs) and their interactions with the blood cells, i.e., platelets, red-blood cells (RBCs) and white cells (WCs).*

**The Role of Cells:** Histological observations have revealed a degeneration of ECs and degradation of the intracellular matrix of the arterial walls due to decreasing density of smooth muscle cells (SMCs). WSS is related to the endothelial gene expression, and in laminar flow produces a quiescent phenotype protecting from inflammation or cell apoptosis. However, flow instabilities and oscillatory WSS can trigger certain genetic traits that affect the elastic properties of the arterial wall. For example, recent studies reported that low WSS levels in oscillatory flow can cause

irregular EC patterns, potentially switching from an atheroprotective to an atherogenic phenotype (Meng et al. 2007, Sforza et al. 2009). On the other hand, low WSS can also be protective as it leads to thickening of arterial walls, which then becomes more tolerant to mechanical loads. Hence, by simply examining the magnitude of WSS we cannot arrive at a consistent theory of aneurysm growth or rupture. To this end, experimental studies with ECs subjected to impinging flow (Meng et al, 2007) have shown the importance of WSS gradients (WSSG) (rather than the magnitude) on the migration of ECs downstream of the stagnation region.

Perhaps the most dramatic evidence on the role of ECs and their interaction with blood cells has been documented in a Japanese clinical study comparing ruptured and un-ruptured aneurysms (Kataoka, 1999). Ruptured aneurysms exhibited significant endothelial damage and inflammatory cell invasion compared with un-ruptured aneurysms; see Figure 2(right) for a typical image. We observe that the EC layer is drastically altered and covered with blood cells and a fibrin network. Similarly, it was reported in (Kataoka, 1999) that *leukocytes* (WCs) in the wall could be associated with SAH, and endothelial erosion enhances leukocyte invasion of the wall before rupture. In addition, the role of RBCs has also been elucidated in recent work in (Cebal et al, 2009): For a basilar artery aneurysm, for which 3D angiographic imaging was made just hours before it ruptured, a patient-specific CFD model was constructed. It was found that a concentrated inflow jet would have impacted onto a small region of the dome of the aneurysm while it remained intact. One of the events likely to affect the hemodynamics in CAs, particularly as they become obstructed with wire coils, is the formation of red-cell rouleaus. In addition, the role of *platelets* has not been fully explored in experimental work, but clinical tests have documented the existence of spontaneous thrombosis in giant aneurysms (Rayz et al, 2008) due to platelet deposition. Thrombus formation within the aneurysm is non-uniform due to the complex flow patterns and the interaction of platelets with the damaged EC layer. Similarly, it was found in endovascular studies that creation of spontaneous thrombosis occurs after stent placement (Vanninen et al, 2003). In other studies, enhanced platelet aggregability has been observed in cerebral vasospasm following aneurysmal SAH (Okhuma et al, 1991).

A *key question* regarding the process of aneurysm progression is how to correlate the blood cell dynamics and interactions to the complex flow patterns observed within the aneurysms. To this end, there are currently two schools of thought: *high-flow* effects and *low-flow* effects (Sforza et al, 2009). The former suggests that localized elevated WSS cause endothelial injury that causes an over-expression of NO production, which in turn can lead to apoptosis of SMCs and subsequent wall weakening. The latter points to the *stagnation* type flow in the dome of the aneurysm, which also causes irregular production of NO. This dysfunction of flow-induced NO leads to *aggregation of red blood cells* as well as accumulation and adhesion of *platelets* and *leukocytes* along the intimal surface (the first layer of the arterial wall). This, in turn, may damage the intima, allowing for infiltration of WCs and fibrin.

**Multiscale Modeling:** Considering the aforementioned findings, simulating the rupture of CAs requires multiscale modeling to account for blood flow in MaN and for explicitly accounting for the presence and interactions of blood cells with the arterial wall as well as cell-cell interactions (e.g. rouleaux formation). To this end, methods similar to the triple-decker algorithm can be employed (Fedosov & Karniadakis, 2009), as shown in the schematic of Figure 3. In particular, a

continuum description (Navier-Stokes) can be employed for the large domain to represent accurately the flow dynamics in the internal carotid artery (ICA) and also downstream of the supraclinoid ICA - including the entire Circle of Willis and other peripheral arteries as needed. On the other hand, the smaller (aneurysm-only) domain will represent the region inside and around the aneurysm, where an atomistic flow description based on the dissipative particle dynamics (DPD) method will be employed. The two domains overlap in order to achieve a seamless representation of the flow and facilitate the introduction and removal of blood cells at the inlet and outlet.

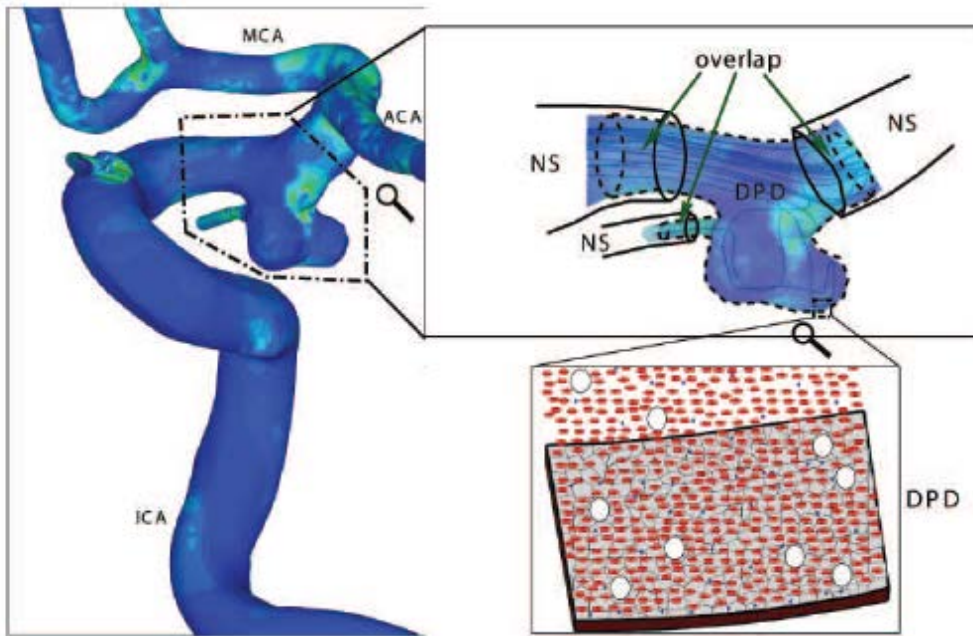


**Figure 3:** *Left: Flow visualization in a aneurysm based on MaN simulations results Right: Proposed multiscale Continuum (NS)--Atomistic (DPD) modeling, showing the two overlapped domains and a sketch of the rheology to be simulated inside the aneurysm that includes red blood cells (red), platelets (blue) and white cells (white). The dynamics of blood cells will be simulated by DPD-LAMMPS.*

## Methods and Integration

**Simulations at the MaN level** involve the solution of the 3D Navier-Stokes equations taking into account the compliance of the large brain vessels. Given proper initial conditions, the system of equations describing the fluid flow in the arbitrary Lagrangian-Eulerian (ALE) reference

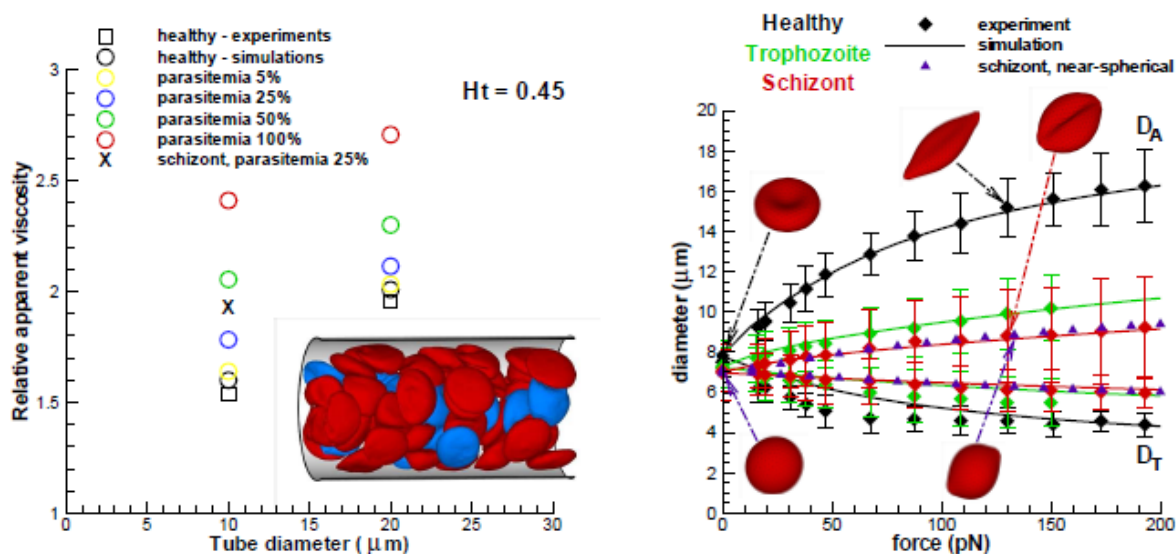


**Figure 4:** Left - Flow resistance in malaria: Healthy (red) and malaria-RBCs (blue) in Poiseuille flow in a arteriole of diameter  $D=20$  microns. The Hematocrit is 45%, and the parasitemia level is 25%. Plotted is the relative apparent viscosity of blood in malaria for various parasitemia levels and tube diameters. Symbol ``x'' correspond to the schizont stage with a near-spherical shape. Experimental data from the empirical fit by Pries et al. (1992). Right - Increased stiffening of malaria-infected RBCs: Simulated stretching of healthy and malaria-infected RBCs at different malaria stages compared with optical tweezers experiments of Prof. S. Suresh.  $D_A$  and  $D_T$  refer to the axial and transverse diameters.

frame can be solved with any type of CFD methods, e.g. finite elements. This should be coupled to hyper-elasticity equations governing the displacements of the flexible arteries and the aneurysmal domain. The fluid and solid domains are coupled through proper kinematic and dynamics boundary condition at the interface. Modeling of this fluid-structure interaction (FSI) is a major challenge cutting across many diverse areas of biomedical modeling.

**At the MeN level**, the quasi-1D Euler hyperbolic equations can be employed accounting also for the dynamic motions of the arteriolar tree (Sherwin et al, 2003). The mathematical model is based on the nonlinear 1D equations for pressure and for the flow wave propagation in compliant vessels. They express conservation of mass and momentum but they are averaged over the cross-sectional. Solution of this system can also be solved using any CFD method for hyperbolic systems, e.g. finite volumes or discontinuous Galerkin methods. Due to the statistical description of the arteriolar tree but also because of *uncertainties* in its material properties, a stochastic modeling approach based on generalized polynomial chaos can be followed (Xiu & Karniadakis, 2002). This approach has been found to be very effective for a moderate number of uncertain parameters with a speed-up factor compared to Monte-Carlo simulation greater than 1,000.

**At the MiN level**, mesoscopic methods such as coarse-grained MD or Lattice Boltzmann or the dissipative particle dynamics (DPD) can be employed. In particular, DPD has already been used

with success in modeling explicitly platelets and red blood cells, e.g. Fedosov et al. (2010). It is based on coarse-graining of MD, with each particle representing a molecular cluster rather than an individual molecule (Lei & Karniadakis, 2010). The DPD system consists of  $N$  point particles, which interact through conservative, dissipative and random forces given forming a system of stochastic ODEs, which are solved with extensions of MD methods. DPD has been implemented in the popular MD code LAMMPS by Sandia Labs. An example is shown in Figure 4, where healthy red blood cells and malaria-infected red blood cells are modeled.

**Integration across scales**, e.g. coupling MaN-MeN or MaN-MiN or of all vascular networks simultaneously depending on the biomedical problem we need to model, should be based on proper interface conditions so that mass and momentum (and possibly energy) are conserved. There have been many attempts in the literature to couple continuum with molecular dynamics directly both for fluids and solids but they have not been adopted for production computing due to the complexity of the algorithms and the apparent errors at the interface. In contrast, interfacing mesoscopic methods with continuum is more appropriate and conservation laws can be readily maintained with the proper use of microscopic forces and torques, e.g., see Fedosov & Karniadakis for a description of a triple-decker algorithm (2009). There are many challenges remaining that have to be addressed in the specific context of modeling biomedical problems.

## References

- Baek, H. et al, Flow instability and wall shear stress variation in intracranial aneurysms, *J. Royal Society, Interface*, vol. 7, pp. 967-988, 2010.
- Baek, H. et al, Distribution of WSS on the internal carotid artery with an aneurysm: A CFD sensitivity study, *Proceedings of IMECE2007*, November 11-15, Seattle, USA, 2007.
- Cassot, F. et al, A novel three-dimensional computer-assisted method for a quantitative study of microvascular networks of the human cerebral cortex, *Microcirculation*, vol. 13, pp. 1-18, 2006.
- Cebral, J.R. et al, Hemodynamics in a Lethal Basilar Artery Aneurism Just Before its Rupture, *Amer. J. Neuroradiol.*, vol. 30, pp. 95-98, 2009.
- Chien, S. et al., Viscoelastic properties of sickle cells and hemoglobin, *Blood Cells*, vol. 8, pp. 53-64, 1982.
- Fedosov, D. and Karniadakis, G.E., Triple-Decker: Interfacing atomistic-mesoscopic-continuum flow regimes, *J. Comp. Phys.*, vol. 228, pp. 1157-1171, 2009.
- Fedosov, D. et al., Systematic coarse-graining of spectrin-level red blood cell models, *Computer Methods in Applied Mechanics and Engineering*, vol. 199, pp. 1936-1948, 2010.
- Grinberg, L. et al, Simulation of the human intracranial arterial tree, *Philosophical Transactions of the Royal Society A*, vol. 367, pp. 2371-2386, 2009.

- Kataoka, K. et al, Structural fragility and inflammatory response of ruptured cerebral aneurysms, *Stroke*, vol. 30, pp. 1396-1401, 1999.
- Kaul, D.K. and Fabry, M.E., In vivo studies of sickle red blood cells, *Microcirculation*, vol. 11, pp. 153-165, 2004.
- Lasheras, J.C., The Biomechanics of Arterial Aneurysms, *Annu. Rev. of Fluid Mech.*, vol. 39, pp. 293-319, 2007.
- Lei, H. and Karniadakis, G.E., Direct construction of mesoscopic models from microscopic simulations, *Physical Review E*, vol. 81, p. 026704, 2010.
- Mayerich, D. et al, Knife-edge scanning microscopy for imaging and reconstruction of three-dimensional anatomical structures of the mouse brain, *Journal of Microscopy*, vol. 231, pp. 134-143, 2008.
- Meng, H. et al, Complex hemodynamics at the apex of an arterial bifurcation induces vascular remodeling resembling cerebral aneurysm initiation, *Stroke*, vol. 38, pp. 1924-1931, 2007.
- Okhuma, H., et al, Role of platelet function in symptomatic cerebral vasospasm following aneurysmal subarachnoid hemorrhage, *Stroke*, vol. 22, pp. 854-859, 1991.
- Pries, A.R. et al, Blood viscosity in tube flow: dependence on diameter and hematocrit, *American Journal of Physiology*, vol. 263, pp. H1770-H1778, 1992.
- Rayz, V.L. et al, Numerical simulation of cerebral aneurysm flow: Prediction of thrombus-prone regions, *Proc. 8th World Congress on Computational Mechanics (WCCM8)*, June 30 July 5, Venice, Italy, 2008.
- Sforza, D.M. et al, Hemodynamics of Cerebral Aneurysms, *Annu. Rev. of Fluid Mech.*, vol. 41, pp. 91-107, 2009.
- Sherwin, S.J. et al., 1D modelling of a vascular network in space-time variable, *J. Eng. Math.*, vol. 47, pp. 217-250, 2003.
- Vanninen, R. et al, Broad-based intracranial aneurysms: Thrombosis induced by stent placement, *AJNR Am. J. Neuroradiol.*, vol. 24, pp. 263-266, 2003.
- Xiu, D. and Karniadakis, G.E., The Wiener-Askey polynomial chaos for stochastic differential equations, *SIAM J. Sci. Comput.*, vol. 24, pp. 619--644, 2002.
- Zamir, M., On fractal properties of arterial trees, *J. Theor. Biol.*, vol. 197, pp. 517-526, 1999.

## Appendix C:

### **Micro-scale Transport as a Critical Link between Molecular-scale Absorption and Macro-scale Mixing in Gut Physiology and Function**

NSF Award CTS-0506215

James G. Brasseur (PI)

Andrew Webb (Co-PI)

Yanxing Wang, Gino Banco (Computational Models)

Amit Ailiani, Thomas Neuberger (MRI Experiments)

The primary roles of the small intestine (gut) are nutrient absorption and transport of digestive material (chyme). Propulsive wave-like propagations (peristalsis) control axial transport, while rhythmic contractions of short segments of the gut (segmentation) are believed to control radial transport and absorption (Ehrlein et al. 1987, Macagno and Christensen 1980). Once advected to the surface, nutrients must diffuse through a low-velocity diffusion layer known as the “unstirred (water) layer (UL)” (Mailman *et al.* 1990). *In vitro* estimates of the thickness of this layer has been reported up to ~1000  $\mu\text{m}$  (Thomson and Dietschy 1984), however these are mechanically unrealistic. Using more accurate methods *in vivo*, however, thicknesses less than 50 $\mu\text{m}$  have been reported, suggesting the existence of a “highly efficient stirring mechanism” (Strocchi and Levitt 1991, Levitt et al. 1992). We hypothesized that the motility of finger-like projections called villi (Womack *et al.* 1989) on the mucosal surface may be responsible. A schematic of a villus is shown in Fig. 1. Since it has not been possible to measure villi motion *in vivo*, we study the potential micro-macro scale transport physics through a series of functionally relevant computational models. The models apply the lattice Boltzmann (LB) framework to predict fluid motions (Chen and Doolen 1998, Succi 2001), nutrient concentration transport using the “moment propagation method” (Merks *et al.* 2002) and absorption with second order moving boundary conditions on momentum (Ladd 1994, Lallemand and Luo 2003) and second order zero-concentration at the epithelial surfaces to model rapid nutrient absorption (Wang *et al.* 2010). We also apply a multi-lattice strategy (Yu *et al.* 2002) to couple numerically the macro and micro scales. The details of the numerical method with higher order boundary conditions, scalar concentration transport, and the macro-micro multi grid strategy is described and validated in a recent publication by Wang *et al.* (2010).

We began our study with two-dimensional (2-D) models (Wang *et al.* 2010, Banco 2010). The first is a lid-driven cavity flow with 2-D “villi” lining the bottom designed to analyze the fluid dynamics by which disparate macro-micro scale motions might interact dynamically to alter of nutrient transport and absorption (Fig. 1). The second is a 2-D macro-scale gut model of fluid motion and nutrient transport and absorption generated by peristaltic and segmental motility where the relative mixes of peristalsis and segmental motility were systematically changed. This model was integrated with magnetic resonance imaging data from the rat intestine *in vivo* (Ailiani et al. 2009) and was subsequently generalized to a three dimensions.

There exists a broad literature on models for transport with peristalsis in biological systems (Li and Brasseur 1993, Li *et al.* 1994), however little is understood about segmental contractions which are prevalent in the gut (Ehrlein et al. 1987). With the macro-scale motility models (Banco

2010) we show that the absorption dynamics of the small intestine at the macro scale is much more complex and interesting than is described in the literature. Common wisdom associates segmentation with absorption and peristalsis exclusively with transport. In contrast both peristalsis and segmentation significantly promote nutrient absorption. However, to maximize absorption while minimizing the power required by the muscles to generate the gut motility, segmentation is optimal over the range of functionally relevant occlusion ratios.

To study the interactions between macro-scale eddying motions and a micro mixing layer generated by villus motility, a multi-grid lattice Boltzmann model was developed with second order moving boundary conditions for lid-driven cavity with villi lining the lower surface as illustrated in Fig. 1 with results from Wang *et al.* (2010) in Fig. 2. The initial 2-D model with 2-D “villi” was subsequently generalized to a 3-D cavity flow model with finger-like villi, more representative of the human gut (Banco 2010). Results of the 3-D simulation are shown in Fig. 3. We show that coordination between the outer macro-scale eddying motion and an inner micro-mixing layer (MML), generated by specific patterning of villi, create advection-dominated macro and micro scale layers separated by an internal micro-scale diffusion layer that work together to enhance the rate of transport of nutrients to the epithelium. The strength of the MML is associated with vertical ejections of low concentration fluid from between villi groups and absorption enhancement results from the return of high-concentration fluid to the villi surfaces from the diffusion layer. Three-dimensional motions reduce the strength of the MML while enhancing absorption over the legs of the villi (Fig. 3).

The previous knowledge and model strategies were combined in the design of a three-dimensional, multi-scale lattice Boltzmann model of the intestine with villi lining the intestinal wall (Fig. 4) to study the effects of coupled macro-scale deformations and pendular villous motility on absorption in the gut (Banco 2010). These are massive high-performance computing simulations requiring TeraGrid resources. We show that active movements of the villi can enhance absorption by 25% above that with passive villous movements that are a result of macro-scale motility patterns alone. Increasing the length or the frequency of oscillation enhances the effect. Consistent with the findings of our lid-driven cavity flow villous motility models, we show that the presence of coordinated counter-oscillating groups of villi is a key mechanism in generation of the MML, and significantly promotes absorption. Azimuthally moving counter-oscillating groups of villi are most advantageous to absorption. Because the azimuthal movements are perpendicular to the fluid patterns induced by the macro-scale motility, the interaction produces 3-D fluid motions that further enhance mixing and increase the absorption in the gut. As shown in Fig. 5, the overall conclusion is that microscale-macro-scale interactions associated with the generation of micro-scale mixing motions by villi motility can both enhance and control absorption of nutrients (and pharmaceuticals) in the intestine.

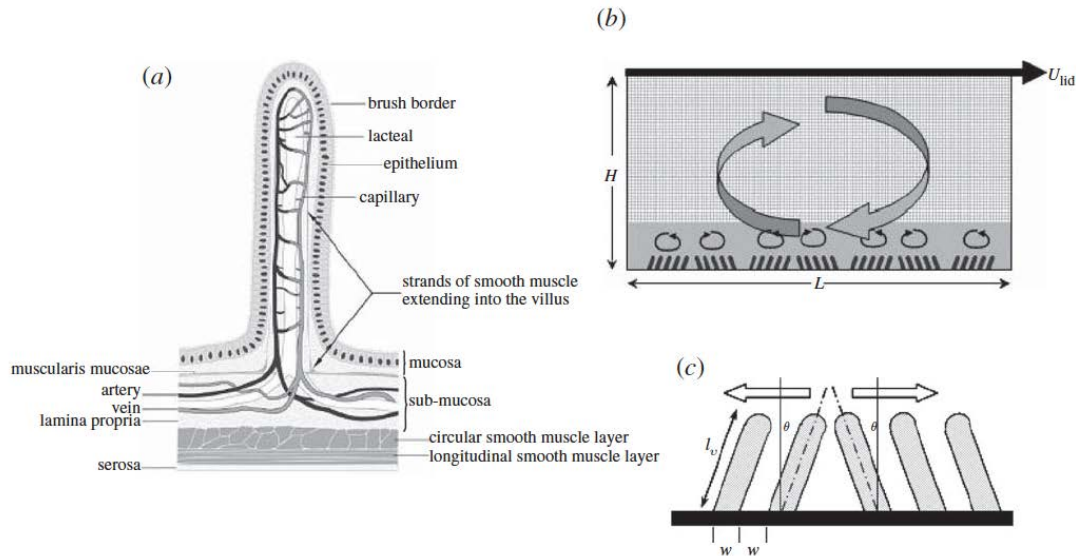


**Figure 1:** (a) A single finger-like human villus (from DeSesso & Jacobson, *Food Chem. Toxicol.* **39**, 209–228, 2001). (b) The multiscale lattice numerical model for studying macro–micro-scale interactions: a two-dimensional lid-driven cavity flow with groupings of ‘villi’ at the lower surface. The fine lattice covers the villi while the coarse lattice covers the rest of the domain. (c) Specification of villi geometry and motion. (Wang et al. 2010)

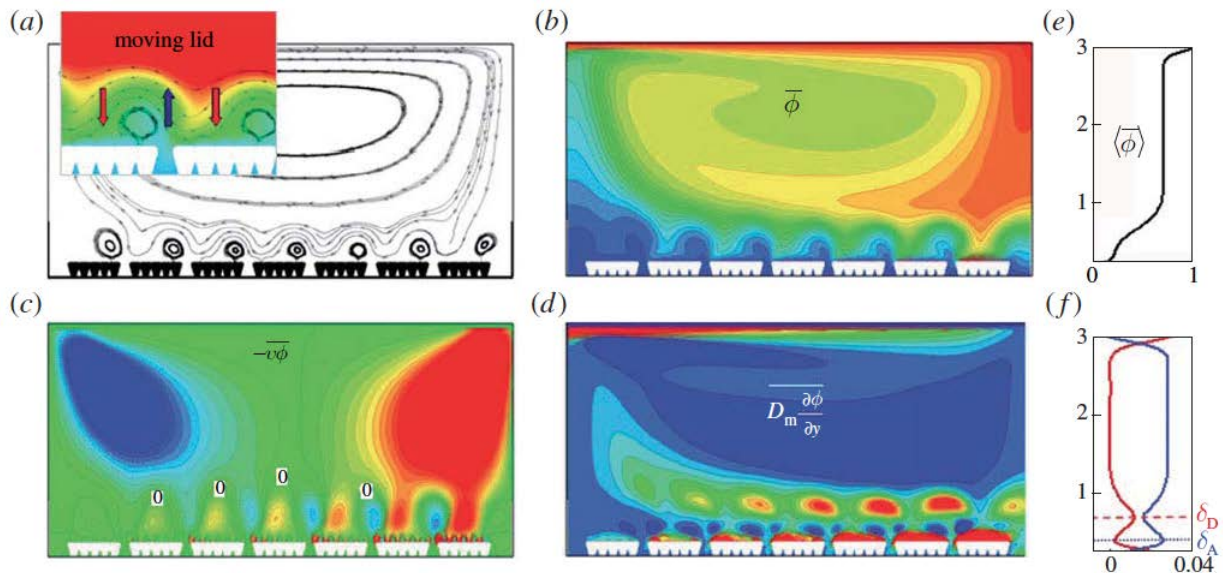


**Figure 2:** Fields averaged over one period of villi motion with moving lid. (a) Streamlines. (b) Isocontours of the molecular concentration field. (c) Vertical concentration flux by advection. (d) Vertical concentration flux by diffusion. (e) and (f) show time-averaged fluxes averaged again over horizontal planes: (e) concentration, (f) vertical concentration flux by advection (blue) and by diffusion (red). Flux is defined positive from the outer flow towards the villi. In the isocontours, high or positive values are red while low or negative values are blue. Zero values in (c) and (d) are green. The inset in (a) shows average streamlines overlaid with concentration

isocontours. Villus length =200  $\mu\text{m}$  and villus-to-outer frequency ratio =40. (Wang et al. 2010)

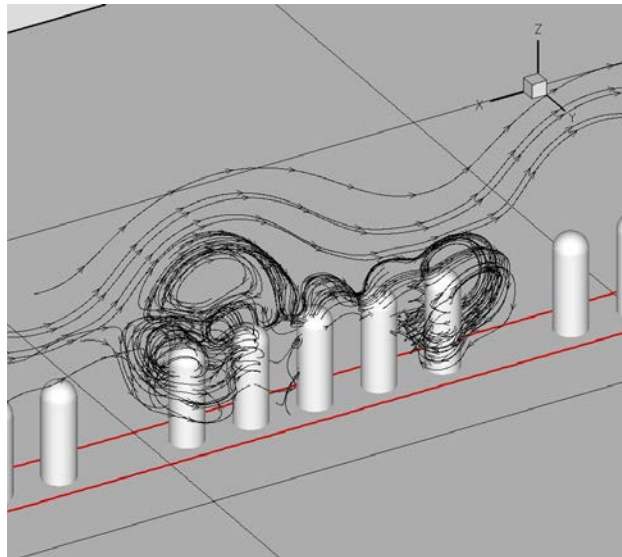


**Figure 3:** Streamlines formed by the interaction between the flows generated by villous motility and macro-scale circulation. The streamlines wrap around the villi moving nutrient molecules into the intravillous spaces.

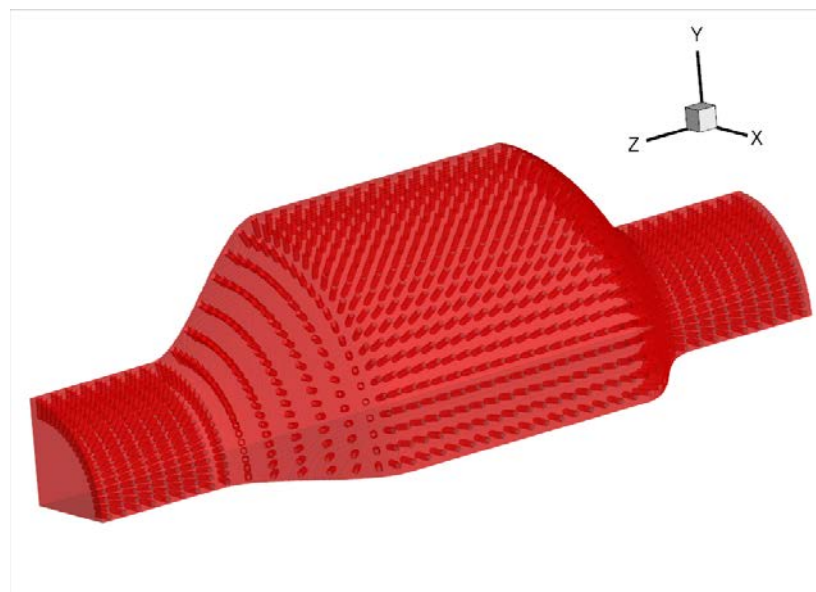


**Figure 4:** Combined multi-scale model of both macro-scale intestinal motility and micro-scale oscillatory villous motility. Segmental intestinal motility with 960 villi is shown.

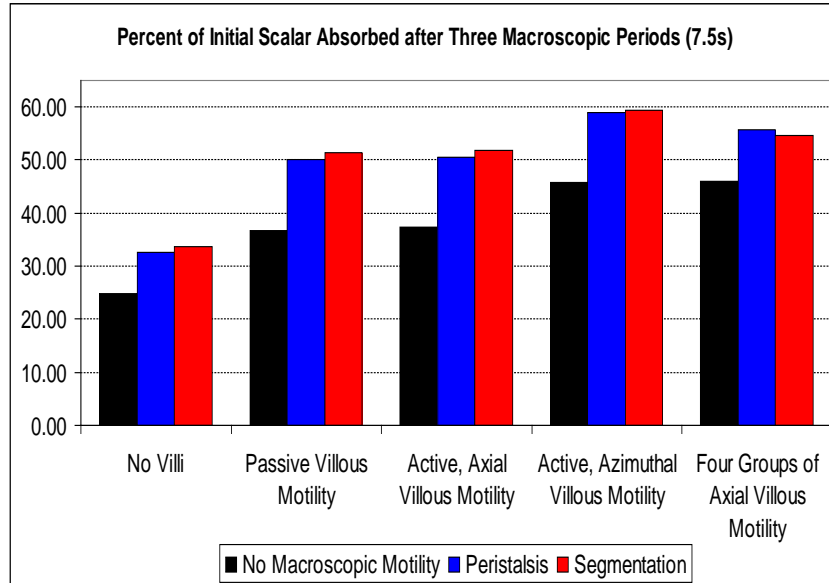


**Figure 5:** Percent of initial amount of scalar (nutrients) absorbed after three macro-scale motility periods (7.5s) for various cases. The black bars represent cases with no macro-scale motility; the blue bars represent cases with peristaltic macro-scale motility; the red bars represent cases with segmental motility. The bar groups represent different cases of villous motility, as indicated by the labels below the groups.

## References:

- Aliani, A.C., Neuberger, T., Banco, G., Wang, Y., Smith, N., Bresseur, J.G., and Webb, A.G., 2009. Quantitative Analysis of Peristaltic and Segmental Motion *in-vivo* in the Rat Small Intestine Using Dynamic MRI. *Magn. Reson. Med.* 62, 116–126.
- Banco 2010 *Multi-scale fluid mechanics of nutrient absorption in the small intestine analyzed with 2D and 3D lattice Boltzmann models*. PhD Thesis, Department of Mechanical and Nuclear Engineering, The Pennsylvania State University.
- Chen, S., Doolen, G.D., 1998. “Lattice Boltzmann method for fluid flows.” *Annual Review of Fluid Mechanics*. 30: 329–364.
- Ehrlein, H.J., Scheman, M., and Siegle, M.L., 1987. “Motor patterns of small intestine determined by closely extraluminal transducers and videofluoroscopy.” *American Journal of Physiology, Gastrointestinal and Liver Physiology* 253 (3), G259-G267.
- Ladd, A.J.C., 1994. “Numerical simulations of particulate suspensions via a discretized Boltzmann-equation. Part 1. Theoretical foundation.” *Journal of Fluid Mechanics* 271: 285–309.
- Lallemand, P., and Luo, L., 2003. “Lattice Boltzmann method for moving boundaries.” *Journal of Computational Physics* 184, 406–421

- Lammers, W.J.E.P., Lammers-van den Berg, A.M., Morrison, J.F.B., and Petroianu, G.A., 2006. "Translating Trendelenburg; back to the future." *Naunyn-Schmiedeberg's Archive of Pharmacology* 373: 134-138
- Levitt, M.D., Stocchi, A., and Levitt, D.G., 1992. "Human jejunal unstirred layer: evidence for extremely efficient luminal stirring." *American Journal of Physiology* 262(25): G593-G596.
- Li, M.J., Brasseur, J.G., 1993. "Non-steady peristaltic transport in finite length tubes." *Journal of Fluid Mechanics* 248, 129-151.
- Li, M.J., Brasseur, J.G., and Dodds, W.J., 1994. "Analyses of normal and abnormal esophageal transport using computer-simulations." *American Journal of Physiology* 266 (4), G525–G543.
- Macagno, E.O., Christensen, J., 1980. "Fluid mechanics of the Duodenum." *Annual Review of Fluid Mechanics* 12, 139-158.
- Mailman, D., Womack, W.A., Kvietys, P.R., and Granger, D.N., 1990. "Villous motility and unstirred water layers in canine intestine." *American Journal of Physiology* 258: G238-G246.
- Merks, R.M.H., Hoekstra, A.G., and Sloot, P.M.A., 2002. "The Moment Propagation Method for Advection-Diffusion in the Lattice Boltzmann Method: Validation and Péclet Number Limits." *Journal of Computational Physics* 183, 563-576.
- Stocchi, A., and Levitt, M.D., 1991. "A Reappraisal of the Magnitude and Implications of the Intestinal Unstirred Layer." *Gastroenterology* 101: 843-847.
- Succi, S., 2001. The Lattice Boltzmann Equation for Fluid Dynamics and Beyond. Numerical Mathematics and Scientific Computations. Oxford Science Publications.
- Thomson, A.B.R., and Dietschy, J.M., 1984. "The Role of the Unstirred Water Layer in Intestinal Permeation." *Handbook of Experimental Pharmacology* 70(II): 165-259.
- Wang, Y., Brasseur, J.G., Banco, G.G., Webb, A.G., Aliani, A.C., Neuberger, T. 2010. Development of a Lattice-Boltzmann Method for Multiscale Transport and Absorption with Application to Intestinal Function. In: Suvarnu D., Farshid, G., Mofrad, M. R. K. (Ed.), Computational Modeling in Biomechanics. Springer. Ch. 3. 69-96.
- Wang, Y., Brasseur, J.G., Banco, G.G., Webb, A.G., Aliani, A.C., Neuberger, T. 2010. "A multiscale lattice Boltzmann model of macro- to micro-scale transport, with applications to gut function." *Phil. Trans. R. Soc. A.* 368, 2863-2880.
- Womack, W.A., Kvietys, P.R., and Granger, D.N., 1989. "Villous Motility". *Handbook of Physiology, The Gastrointestinal System I* p.975-985.
- Yu, D., Mei, R., Shyy, W., 2002. "A multi-block lattice Boltzmann method for viscous fluid flows." *International Journal for Numerical Methods in Fluids.* 39: 99-120.

## Appendix D:

### Multiscale Aspects of Modeling Tumor Growth

Yi Jiang, Los Alamos National Laboratory

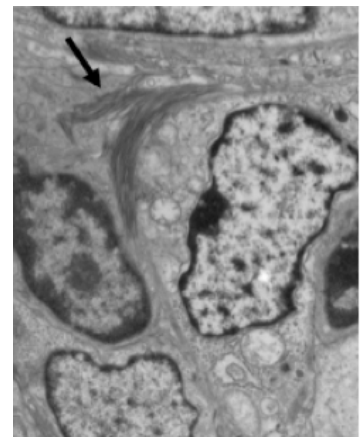
Bridget Wilson, University of New Mexico

The goal of this white paper is to explore important issues related to developing multiscale models of tumor development, using “cell-based” models.

#### **Premise 1. Multiscale models of mechanics of cell and tissue, especially cell migration in a 3D tissue context, will require multi-physics, multi-model integration.**

While several multiscale models of tumor development exist (e.g. 1-7), none is able to incorporate realistic biomechanics. The integration of biomechanics into the existing frameworks is the crucial next step to make these models truly predictive.

One important aspect of tumor growth microenvironment is the extracellular matrix (ECM). This matrix can serve many functions, including providing support and anchorage for cells, segregating tissues from one another, and regulating intercellular communication. The ECM also regulates a cell's dynamic behavior, particularly in the context of tumor metastasis and invasion. Dense breast tissue is a strong and frequent risk factor for the development of invasive breast cancer and is associated with excess collagen deposition. Transgenic mouse tumor studies indicate that excess collagen does promote both tumor formation and invasiveness, although the mechanism is unclear. In addition, alignment of collagen fibers in tumors correlates strongly with tumor invasion, suggesting that reorganization of the dense matrix by tumor cells is involved in the invasive phenotype. One potential explanation is that dense matrix triggers mechanotransduction signaling responses in tumor cells, leading to contraction and alignment of collagen fibers and subsequent migration by tumor cells. However, it is also possible that the dense, aligned matrix is associated with other tumor features, such as fibroblast recruitment that promotes tumor progression through other mechanisms. Moving beyond correlative data and understanding the underlying mechanisms is difficult using traditional experimentation alone, since extracellular matrix (ECM) affects many aspects of both host and tumor cell behavior, including migration, invasion, and proliferation. Furthermore, the properties of ECM itself are also complex, with diverse topographies and mechanical properties possible depending on the density, alignment, polymerization, and crosslinking.



Transmission electron micrograph illustrating collagen deposits (arrow) between cells in an ovarian tumor (xenograft model; unpublished observations, Wilson laboratory).

It would be very desirable and important to understand the role of ECM mechanics in tumor cell. We therefore propose to use a first principles approach in which we use mathematical modeling to test in silico the role of specific aspects of ECM tumor interactions in tumor progression. Using such an approach, we can isolate variables and explore quickly a wide parameter space in silico.

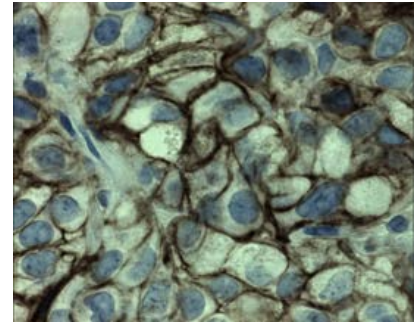
We have developed a cell-based, multiscale modeling framework that have successfully simulated avascular tumor growth (2) and tumor angiogenesis (8). Both are based on the Cellular Potts Model (CPM, also called GGH model) (9). The discrete Monte Carlo lattice-based model partitions 2D or 3D space into domains that represent tumor cells and generalized “cell” features such as interstitial fluid or basement membrane. Every “cell” has a unique ID number, which occupies all the lattice sites within the cell domain, so it has a finite volume and a deformable shape. “Cells” have direct contact and interact with each other through surface adhesion and competition for space. Interactions are characterized through total system energy, which includes an adhesion energy term between cells, a volume energy for cells and a continuity constraint applied to migrating tumor cells to prevent nonbiological fragmentation. The extracellular chemical microenvironment includes nutrients (oxygen and glucose), metabolic waste, and growth factors. Oxygen and glucose are supplied by the external microenvironment. The growth factors and inhibitors are produced by cells. All chemicals follow the reaction-diffusion dynamics.

An important **multiscale** aspect of the current model is the inclusion of an intracellular regulatory network, representing the cell cycle. Incorporation of this Boolean network allows natural emergence of the cell phenotypic outputs of quiescence and necrosis and has been shown to match experimental results in a tumor spheroid model. The three levels are closely integrated through information flow between the levels. The tumor in our simulation starts from a single tumor cell in the center of the medium, and grows into a spheroid tumor consisting of proliferating and quiescent cells surrounding a necrotic core (2). Intracellular regulatory networks can be extended to other important cellular fate decisions, such as programmed cell death or response to external stimuli, by incorporating specific signaling pathways.

To date, our model of cell-stroma interactions during the early stages of VEGF-induced angiogenesis has been based in 2D space (8). The ECM was treated explicitly as a matrix of fibers, with the interstitial fluid filling the space between the cells and the fibers. Activated endothelial cells proliferate and migrate chemotactically up a VEGF gradient. The model is able to capture realistic cell dynamics and capillary morphologies, such as preferential sprout migration along matrix fibers and cell elongation, and more complex events, such as sprout branching and fusion, or anastomosis, that occur during angiogenesis. We have also investigated possible mechanisms for sprout branching by changing the stromal composition. The results suggested that local heterogeneities in the stroma, such as matrix fiber density and the presence of stromal cells, promote sprout branching and anastomosis. The capillary branching behavior in simulations emerged naturally from the cell-matrix and cell-cell interactions in the model. We varied the

density of matrix fibers and found specific ranges of matrix fiber densities that maximize sprout extension speed, induce branching, or interrupt normal angiogenesis (10). The limitation of modeling cell-matrix interactions in 2D is that it cannot accurately model 3D ECM topography, including spatial constraints that would prevent migration in tissues. The effects of ECM density in 2D models are primarily a function of changes in adhesive strength, similar to what is seen in 2D in vitro migration studies.

Another important consideration is the variability of cell-cell adhesion complexes between cells in solid tumors. These interactions are maintained by surface receptors, including integrins and components of tight junctions, adherens junctions, desmosomes and even gap junctions. This is illustrated in the figure at right, where the brown stain indicates the locations where homotypic interactions between E-cadherin molecules serve as the “glue” between tumor cells. Integrate features of cell-cell adhesion receptors (integrins) and junctional proteins into the intracellular regulatory network that will govern behavior of individual cells in tumors with respect to maintaining cell-cell aggregation, release and migration away from the primary site and attachment to new sites. These are crucial features of the metastatic process and are also closely linked to cell proliferation rates. Of particular interest is the crosstalk between the cadherin and the integrin signaling pathway (e.g. 11,12). Hence the cell-cell and cell-matrix interactions are interdependent, and models of biomechanics in multiple cell system would need to take both into account.



E-cadherin labeling of ovarian tumor xenograft tissue shows variability in cell-cell adhesion complexes (Wilson, unpublished results).

In order for the tumor modeling community to address the realistic biomechanics of cell-matrix and cell-cell adhesive interactions, new approaches need to be developed that incorporate 3D cell-ECM interactions. We propose to integrate the ECM mechanics model with the cell-based models with cell adhesion regulation. The CPM framework, where cell type dependent adhesion is already part of its standard feature, can readily accommodate cell adhesion regulation. There are several different ways to couple ECM mechanics of CPM.

1. Use a continuous model to describe the ECM mechanics, e.g. a Kelvin–Voigt model, for linear viscoelasticity; volume exclusion between fibers and cells is more difficult.
2. Use a discrete model of ECM, such as a network of worm-like-chains or elastic springs wherein the interactions are explicit force balance equations; solutions to the force equations approximate the force and deformation of the fibers.
3. Use a discrete model of ECM within the Cellular Potts Model framework wherein the interactions are described by an effective energy. Some other cell-based models, e.g. the cell-center model based on force calculations, will be able to treat the force coupling between ECM and cell more easily, but the consideration of volume exclusion and cell adhesion will be more tricky.

**Premise 2. Improved cell-based models of tumor growth are needed to consider fluid and molecular transport in the heterogeneous environment, especially in the context of drug delivery to tissue and organ**

Models that incorporate fluid and molecular transport within the tumor and surrounding tissues will be crucial to understanding role of the tumor microenvironment in tumor growth and survival, as well as the accessibility to therapeutic agents.

If we are considering transport through blood, or lymph flow, at low shear rates or in relatively large vessels, fluids behave rheologically as a Newtonian fluid. Therefore, they should be treated as an incompressible fluid with constant viscosity. Namely, we should use the following Navier–Stokes equations:

$$\frac{\partial \mathbf{u}}{\partial t} + (\mathbf{u} \cdot \nabla) \mathbf{u} = \frac{1}{\rho} [-\nabla p + \mu \nabla^2 \mathbf{u} + \mathbf{f}]$$
$$\nabla \cdot \mathbf{u} = 0,$$

where  $\mathbf{u}$  is the flow velocity;  $\rho$  is the density of the fluid; and  $p$  is the pressure. The viscosity  $\mu$  is assumed to be constant.  $\mathbf{f}$  is the force density due to cell-interactions.

On the other hand, when we are considering transport of macromolecules through tissue, then the penetration is dominated by diffusion process:

$$\frac{\partial C}{\partial t} = D \nabla^2 C - \gamma C + \alpha - \beta$$

where  $C$  is the concentration field, and the dynamics include diffusion, decay, source and sink (uptake) terms.

In considering aspects of drug delivery to tumors, it will be necessary to combine aspects of both scenarios. For example, therapeutic agents are typically delivered either orally or by injection, depending on their size, hydrophobicity and requirement for specific transport mechanisms. Initial transport may be through blood or other body fluid flow, followed by penetration into tumor tissue. Parameters for these processes are hard to obtain and scattered in the literature. There is some utility for “phenomenological models”, to get around some parameter shortage and help to constraint the parameter space. Nevertheless, accurate simulation of these processes will remain critically depend on high quality data that is specifically acquired for the modeling effort. This is the most important argument for forming strong interdisciplinary teams, composed of computational biologists, bench scientists and animal model experts. Our own MSM group is committed to this type of effort.

**Premise 3. Sensitivity analysis can identify most critical aspects where experimental data is needed and reduce uncertainty in quantification of system level outputs**

Whenever there are estimated parameters or phenomenological assumptions, uncertainty arises, and must be quantified in order for results to have predictive value. One way to attenuate this uncertainty is to develop methods for information-passing that quantify data variance. For complex systems, it is insufficient to analyze system sensitivity by varying each parameter one at a time and holding all others fixed, because often changes in one parameter effect changes in another; that is they are not independent, or worse, are highly nonlinear. For example, in the cellular Potts model, parameters for membrane elasticity, adhesion strength, and chemotactic potentials are relative parameters, chosen to reproduce cell-level phenomenology. This type of parameter estimation introduces uncertainties into the system. The challenge here is to identify the parameter combinations responsible for given results or outcomes. In a particular application, e.g. tumor spheroid growth, we can use key model outputs, such as tumor growth rate, necrotic core size, cell cycle fraction distribution, to map out the parameter space. The technique of choice would be the Latin hypercube sampling method to quantify the sensitivity of these key model outputs to parameter choices. The advantage of this technique is that it can quantify sensitivity by taking into account the influence of multiple parameters. We can perform a number of simulations over systematically perturbed parameter ranges to statistically characterize key physical parameters. We can average these statistical distributions over the course of each simulation and across simulations to derive error bars for our statistical descriptions in space and time. As we obtain more sample observations, the variance of the distributions will converge in time. By performing a sensitivity and uncertainty analysis of the model's outputs, we will be able to identify key parameters that are responsible for most of the outcome uncertainty. One goal is to use this information to focus the resources of the bench scientists on team, in order to design experiments that provide quantitative data for the most important aspects of the model. Identifying collections of parameter ranges that contribute to a specific system behavior may lead to increased understanding of interacting or competing mechanisms, such as cell migration versus adhesion, as well as parameter correlations.

## References:

1. Alarcón T, Byrne HM, Maini PK. Towards whole-organ modelling of tumour growth. *Prog Biophys Mol Biol.* 2004. 85:451-72. Review.
2. Jiang Y, Pjesivac-Grbovic J, Cantrell C, Freyer JP. A multiscale model for avascular tumor growth. *Biophys J.* 2005. 89:3884-94.
3. van Leeuwen IM, Edwards CM, Ilyas M, Byrne HM. Towards a multiscale model of colorectal cancer. *World J Gastroenterol.* 2007. 13:1399-407.
4. Zhang L, Strouthos CG, Wang Z, Deisboeck TS. Simulating Brain Tumor Heterogeneity with a Multiscale Agent-Based Model: Linking Molecular Signatures, Phenotypes and Expansion Rate. *Math Comput Model.* 2009. 49:307-319.
5. Macklin P, McDougall S, Anderson AR, Chaplain MA, Cristini V, Lowengrub J. Multiscale modelling and nonlinear simulation of vascular tumour growth. *J Math Biol.* 2009. 58:765-98.
6. Lowengrub JS, Frieboes HB, Jin F, Chuang YL, Li X, Macklin P, Wise SM, Cristini V. Nonlinear modelling of cancer: bridging the gap between cells and tumours. *Nonlinearity.* 2010. 23:R1-R9.

7. Shipley RJ, Chapman SJ. Multiscale modelling of fluid and drug transport in vascular tumours. *Bull Math Biol.* 2010. 72:1464-91.
8. Bauer AL, Jackson TL, Jiang Y. A cell-based model exhibiting branching and anastomosis during tumor-induced angiogenesis. *Biophys J.* 2007. 92:3105-21.
9. Glazier JA and Graner F. Simulation of the differential adhesion driven rearrangement of biological cells. *Phys. Rev. E* 1993. 47: 2128-2154.
10. Bauer AL, Jackson TL, Jiang Y. Topography of extracellular matrix mediates vascular morphogenesis and migration speeds in angiogenesis. *PLoS Comput Biol.* 2009. 5:e1000445.
11. Maria von Schlippe, John F. Marshall, Philip Perry, Michael Stone, Alan Jian Zhu and Ian R. Hart. Functional interaction between E-cadherin and  $\alpha$ v-containing integrins in carcinoma cells. *J Cell Sci.* 2000. 113: 425-437.
12. Jones Tsai and Lance Kam. Rigidity-Dependent Cross Talk between Integrin and Cadherin Signaling. *Biophys J.* 2009. 96: L39-L41.